Optical and molecular characterization of dissolved organic matter (DOM) in the Arctic ice core and the underlying seawater (Cambridge Bay, Canada): Implication for increased autochthonous DOM during ice melting

Simona Retelletti Brogi [a], Sun-Yong Ha [b], Kwanwoo Kim [c], Morgane Derrien [a], Yun Kyung Lee [a], Jin Hur [a,*]

[a] Department of Environment & Energy, Sejong University, Seoul 05006, South Korea
[b] Division of Polar Ocean Science Research, Korea Polar Research Institute (KOPRI), Incheon 21990, South Korea
[c] Department of Oceanography, Pusan National University, 30, Jangjeon-dong, Geumjeong-gu, Busan 46241, South Korea

HIGHLIGHTS

- A comparative study for Arctic sea ice and the underlying seawater DOM
- Multiple DOM analyses including FT-ICR MS and SEC are utilized for the first time.
- A net accumulation of in situ-produced DOM was observed in the ice.
- Large amounts of labile small-sized DOM could be annually released upon ice melting.
- This work provides a new insight into DOM composition changes under ice melting.

GRAPHICAL ABSTRACT
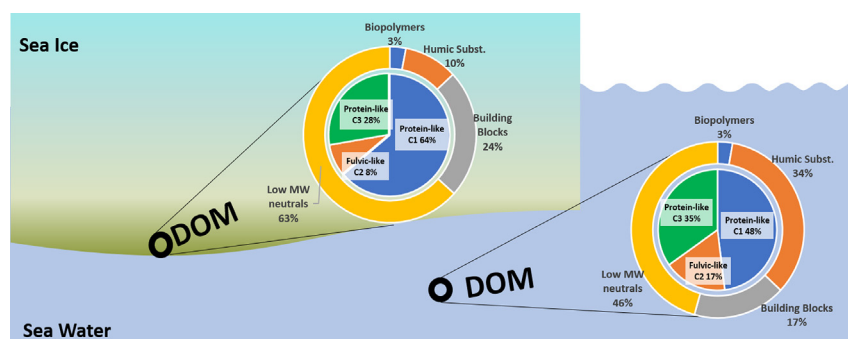
ARTICLE INFO

ABSTRACT

Sea ice contains a large amount of dissolved organic matter (DOM), which can be released into the ocean once it melts. In this study, Arctic sea ice DOM was characterized for its optical (fluorescence) properties as well as the molecular sizes and composition via size exclusion chromatography and Fourier transformation ion cyclotron resonance mass spectrometry (FT-ICR MS). Ice cores were collected along with the underlying seawater samples in Cambridge Bay, an Arctic area experiencing seasonal ice formation. The ice core samples revealed a marked enrichment of dissolved organic carbon (DOC) compared to the seawater counterparts (up to 6.2 times greater). The accumulation can be attributed to in situ production by the autotrophic and heterotrophic communities. Fluorescence excitation emission matrices (EEMs) elaborated with parallel factor analysis (PARAFAC) evidenced the prevalence of protein-like substances in the ice cores, which likely results from in situ production followed by accumulation in the ice. Size exclusion chromatography further revealed the in situ production of all DOM size fractions, with the exception of the humic substance fraction. The majority of DOM in both the ice and seawater consists of low molecular weight compounds (<350 Da) probably derived by the microbial degradation/transformation of freshly produced DOM. Molecular characterization also supported the in situ production of DOM and highlighted the marked difference in molecular composition between sea ice and seawater. This study provides new insights into the possible role of sea ice DOM in the Arctic carbon cycle under climate change.

© 2017 Elsevier B.V. All rights reserved.

* Corresponding author.
  E-mail address: jinhur@sejong.ac.kr (J. Hur).

1. Introduction

As one of Earth's largest exchangeable carbon reservoirs, similar in scale to atmospheric CO_2, marine dissolved organic matter (DOM) and its biogeochemical behavior are of major significance for the carbon cycle, climate, and global habitability. DOM is actively involved in the marine food web as a source of energy for heterotrophic prokaryotes and as byproducts of biological metabolisms (Jiao et al., 2010).

The Arctic Ocean waters contributes to deep water formation in the Northern Hemisphere, and therefore to the dissolved organic carbon (DOC) (>93% of DOM) pool in global deep waters (Anderson, 2002; Anderson and Amon, 2015), while a large fraction of the Arctic DOC pool is stored in sea ice. When ice forms, the DOM, excluded from the crystalline ice structure, accumulates in the liquid brine phase, and 10 to 40% of it can remain trapped in channels within the sea ice (Petrich and Eicken, 2010). The unique Arctic environment, characterized by a low temperature and a high salinity (S > 35), constitute a niche for very productive biological communities (Arrigo, 2016; Deming, 2009). The DOC concentration in sea ice is reported to be typically ~100 μM (Anderson and Amon, 2015). However, in the areas with high biological activity, such as the bottom layer of the ice in the winter-spring season, the DOC levels could reach up to several hundred μM (Thomas et al., 1995). The high DOC concentrations observed in sea ice have been attributed to algal and bacterial production (Aslam et al., 2012; Smith et al., 1997; Underwood et al., 2010; Xie et al., 2014). Such large amounts of DOM are beneficial in mediating the ecology of sympagic organisms (Thomas et al., 2010). The melting of sea ice may therefore be a potential supplier of a significant large amount of labile carbon to the Arctic Ocean. The recent rising trend in sea ice melting during summer, caused by climate change, has led to a marked increase in the areas of the Arctic Ocean that experience seasonal ice melting (Kinnard et al., 2011). This occurrence would facilitate the supply of bioavailable DOC to the Arctic Ocean, and therefore a higher carbon turnover (Jørgensen et al., 2015).

The optical properties of chromophoric DOM (absorption and fluorescence excitation-emission matrices, EEMs) have been extensively used to characterize DOM in sea ice, helping to distinguish between the autochthonous (or biologically derived) fraction and the one that accumulates from the parent seawater, both under natural environments and under laboratory ice-formation experiments (Ehn et al., 2004; Granskog et al., 2005; Hill and Zimmerman, 2016; Jørgensen et al., 2015; Logvinova et al., 2016; Norman et al., 2011; Stedmon et al., 2011, 2007; Xie et al., 2014). Longnecker (2015) reported a more detailed molecular characterization of sea ice DOM by using Fourier transformation ion cyclotron resonance mass spectrometry (FT-ICR-MS). With its ultrahigh mass resolution and accuracy, this technique allows the identification of thousands of compounds and the ability to assign most of them to elemental formulas with a high level of confidence (Repeta, 2015). However, to the best of our knowledge, up to now no studies reported, and compared, fluorescence and FT-ICR-MS data of sea ice together.

The main goal of this study is to characterize DOM in the ice core and the underlying seawater by combining optical and molecular analyses. In addition to the EEMs and FT-ICR-MS, size exclusion chromatography equipped with an organic carbon detector (SEC-OCD) was also utilized, which has a capability to quantitatively separate a bulk DOM sample into several size fractions (biopolymers, humic substances, building blocks, low molecular weight acids, and neutrals) (Huber et al., 2011). For this purpose, ice cores and seawater samples below the ice were collected from the Canada Basin in the proximity of Cambridge Bay. This area was chosen since it is characterized by seasonal ice formation, which is a condition that most resembles the majority of future Arctic ice coverage under climate change effects.

2. Material and methods

2.1. Study area and sampling

The samples were collected on five nonconsecutive days (between April 27th and May 9th) in 2017 from four different stations in the proximity of Cambridge Bay (Nunavut, Canada), which is located between Victoria Island and the Canadian coast (Fig. 1).

In this area, seasonal sea ice formation typically occurs from October until May or June when the ice reaches its maximum thickness of approximately 200 cm (data from Canadian Ice Thickness Program Collection, licensed under the Open Government License – Canada, www.open.canada.ca). The sampling period of this study thus represents the formation of the seasonal thickest ice, just before the melting period. At each station, two types of samples were collected: one from within the ice and one from the seawater below the ice (i.e., the underlying seawater). The ice cores were extracted with an 8 cm-diameter SIPRE ice corer, and the water samples were collected through the small holes. Because most of the biomass is likely concentrated in the lower part of the sea ice, only the bottom 10 cm sections of the sea ice were used for this study. The samples were stored in coolers to avoid light exposure during transfer to the laboratory. Ice core samples were thawed in the dark at room temperature overnight. Before filtration, the samples were homogeneously mixed, and salinity was measured using a YSI model 30 salinity meter (YSI, Yellow Springs, Ohio).

2.2. Analytical measurements

A summary of all the analytical procedures employed, blank collection, reference and standard material used is displayed in Table S1.

Samples for chlorophyll-a (chl-a) concentration were filtered through 0.7 μm pore size filters (Whatman, GF/F). The filters were immediately frozen until analysis. Chl-a was extracted in 90% acetone for 24 h at 4 °C (Parson et al., 1984), and quantified using a pre-calibrated Turner Designs model 10-AU fluorometer. The filtrate was used for the following DOM analyses.

Dissolved organic carbon (DOC) and total dissolved nitrogen (TDN) were quantified by using a total organic carbon analyzer (Shimadzu TOC-VCPH) with an analytical reproducibility <2%. Dissolved inorganic nitrogen (DIN) was measured by using a Quaatro Auto analyzer (Bran + Luebbe, Germany) at the National Institute of Fisheries Science (Korea). Dissolved organic nitrogen (DON) was then calculated as the difference between TND and DIN. Fluorescence excitation emission matrices (EEMs) were scanned with a Hitachi F-7000 fluorescence spectrophotometer (Hitachi Inc., Japan). Excitation ranged between 220 and 500 nm with a 5-nm interval, and emission scans were set at wavelengths between 280 and 550 nm every 1 nm. Blank subtraction and Raman peak normalization were performed following the procedures proposed by Murphy et al. (2010). UV absorption coefficients at 254 nm of all samples were below 0.05 cm^{-1}, making inner-filter correction unnecessary (Hur et al., 2008). Parallel factor analysis (PARAFAC) modeling was carried out in MATLAB R2017a (Mathworks, Natick, MA, USA) using the drEEM Toolbox, (Murphy et al., 2013). The validation of the PARAFAC model was made by visual inspection of the residuals, split half analysis, and percentage of explained variance (99.2%).

DOM size fractions were measured by a high-performance liquid chromatography system (S-100, Knauer, Berlin, Germany) equipped with an organic carbon detector (OCD). The detailed analytical procedure is described elsewhere (Chen et al., 2016a; Huber et al., 2011). For this study, the samples collected on May 9th were chosen for the SEC-OCD measurements. The assignments and the quantification of different size fractions, including biopolymer (BP), humic substances (HS), building blocks (BB), low molecular weight neutrals (LMWN), low molecular weight acids (LMWA), were based on an established procedure (Huber et al., 2011) and the in-built software.
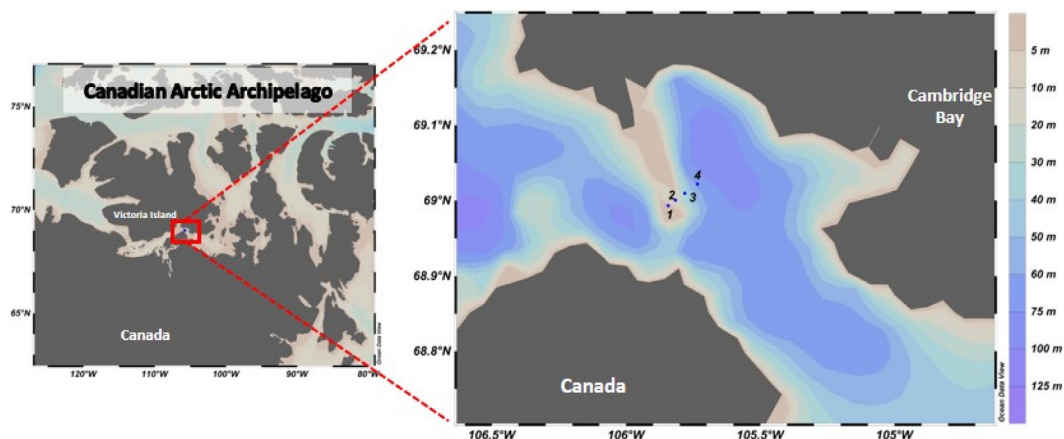
Fig. 1. Sampling area and stations. The maps were created by using Ocean Data View software (Schlitzer R., Ocean Data View, odv.awi.de, 2017).

Molecular composition analysis was carried out using a 15-T FT-ICR MS interfaced with an Apollo II electrospray ionization source (ESI, Bruker Daltonik GmbH, Leipzig, Germany), located at the Korea Basic Science Institute (KBSI) in Ochang (South Korea). A detailed description of the analytical method is given in Derrien et al. (2017a). To ensure a sufficient sample volume for solid phase extraction (SPE), all the collected ice samples and the seawater samples were mixed together to obtain two representative samples for the different environments (i.e., ice and seawater). SPE was performed following the method described in Dittmar et al. (2008) and He et al. (2016). Briefly, the prepacked PPL cartridges (Agilent Bond Elut PPL, Santa Clara, CA, USA) were rinsed with MeOH and Milli-Q water. The acidified samples (pH 2) were passed through the cartridge at 0.5 mL/min and salt was subsequently removed by passing 0.01 M HCl through the SPE system. Finally, the cartridge was fully dried with N_2 and eluted with MeOH. A blank was acquired at the same time following the same procedure by using Milli-Q water. Only the peaks with an S/N > 4 were considered for the MS data acquisition. Molecular formulas were assigned for elemental combinations $^{12}C_{0-\infty}^1 H_{0-\infty}^{16} O_{0-\infty}^{14} N_{0-5}^{32} S_{0-2}$ by using the Composer64 software (Sierra Analytics Inc., version 1.5.4). The mass accuracy threshold was $|\Delta m| \leq 1$ ppm. The nitrogen rule and the double bond equivalent rule (i.e., DBE = 1/2(2C–H + N) ≥ 0) were applied. The elemental ratio criteria were implemented as follows: 0.3 ≤ H/C ≤ 2.25, O/C < 1.2, N/C < 0.5, and S/C < 0.2 to obtain elemental formulas with a high level of confidence, based on the literature (Chen et al., 2016b; Derrien et al., 2017b; He et al., 2016; Koch et al., 2008).

2.3. Statistics

The Kruskal–Wallis test (R software) was used to test the variability between the four sampling stations, and between the ice and the seawater DOM samples. This test was chosen since it is a non-parametric test and does not need any distributional assumption (Sokal and Rohlf, 1995). Differences were considered significant for $p < 0.05$.

3. Results and discussion

For this study, the average values (±standard deviation) of DOC, DON, Chl-a concentrations, and fluorescent DOM (FDOM) components were compared for each sampling station, with a reasonable assumption that there was no major temporal variation within the short sampling period (13 days). For all these parameters, no significant difference was found ($p < 0.05$) between the four stations, both within the ice and the seawater samples. A summary of all the bulk parameters is displayed in Table S2.

3.1. Comparison of DOC, DON, and Chl-a between the ice and the seawater

DOC concentrations of the ice samples ranged between 162 and 640 μM (average: 401 ± 145 μM), while those of the seawater were recorded 6.5 to 6 times lower, ranging between 81 and 213 μM (average: 110 ± 35 μM, Fig. 2a). Such high DOC concentrations in the sea ice have been reported in previous literature on the Arctic and in other polar regions (Meiners et al., 2009; Norman et al., 2011; Stedmon et al., 2011; Thomas et al., 2001, 1995; Underwood et al., 2010). The high DOC concentrations can be explained by the accumulation of a DOM fraction within brine channels during ice formation (Jørgensen et al., 2015; Stedmon et al., 2011, 2007) and subsequent uncoupling between production and removal processes. This uncoupling can be driven by the following processes: (i) the low temperature can affect the substrate affinity of bacteria (Pomeroy and Wiebe, 2001); (ii) the bacteria, mainly attached to particles at low temperatures (Junge et al., 2004), might preferentially utilize the substrates detached from the particles; (iii) bacterial C requirement is only a small fraction (<5%) of the net DOC accumulation (Riedel et al., 2008). It should also be taken into account that the high abundance of DOC in the ice could be attributed in part to some materials released through the breakdown of the cells during the melting procedure.

DON concentrations of the ice ranged between 7.3 and 21.4 μM (average: 11 ± 4 μM), whereas they varied between 2.7 and 12.5 μM in the seawater (average: 6 ± 3 μM, Fig. 2b). These values fall within the DON ranges reported for other polar regions (Meiners et al., 2009; Norman et al., 2011; Stedmon et al., 2011; Thomas et al., 2001). On the contrary to DOC, no significant difference was found between the ice and the seawater DOM, which can be attributed to a larger spatial and temporal variability in DON versus DOC concentrations. Both DOC and DON in the seawater were higher than the average values (54–60 μM and 4.7 ± 1.5 μM, respectively) reported for the Arctic Ocean (Benner et al., 2005; Sipler and Bronk, 2015).

For this study, the DOC:DON ratios ranged between 21 and 57 (average: 40 ± 15) in the ice, and between 7 and 41 (average: 24 ± 8) in the seawater. Such high ratios of DOC:DON, particularly in the ice, were previously reported both in the Arctic and in other polar ice (Norman et al., 2011; Stedmon et al., 2007; Thomas et al., 2001, 1995), and they have been explained by the uncoupling of C and N metabolisms. For example, Thomas et al. (1995) attributed high ratios of DOC/DON to the faster hydrolysis and microbial utilization of N-rich amino acids versus the C-rich polysaccharides pool. Another explanation could be related to the release of C-rich DOM by phytoplankton, induced by nutrient limitations (Carlson and Hansell, 2015).

A larger difference was found in the Chl-a concentrations between the ice and the seawater (31 ± 15 and 1.2 ± 1.5 μg l^{-1}, respectively,
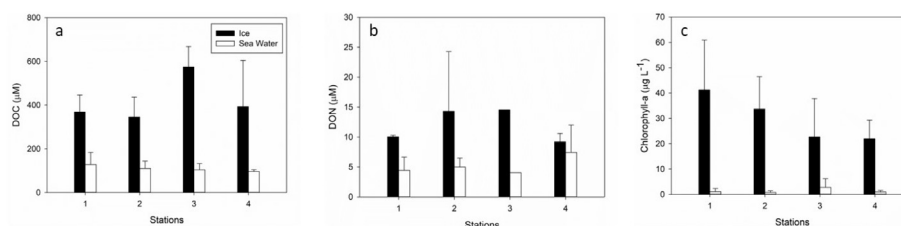
Fig. 2. Dissolved organic carbon (DOC, a), Dissolved organic nitrogen (DON, b), and Chlorophyll-a (c) concentrations in the ice (black) and the seawater (white) at the four stations. Error bars refer to the standard deviation of the samples collected on 5 different sampling days.

Fig. 2c) compared to DOC or DON. The values agreed with the ranges (0–439 and <0.1–13.1 $\mu g \, l^{-1}$ in ice and seawater, respectively) previously reported in polar regions (Granskog et al., 2005; Norman et al., 2011; Thomas et al., 2001). The high Chl-a concentrations of the ice suggest the presence of ice algae and phytoplankton communities, which are particularly abundant in the bottom 20 cm of the ice (Arrigo, 2016; Kaartokallio et al., 2007). Such a high level of algal biomass in the

bottom layer of sea ice, together with the ice itself, likely limits the availability of light for the primary production of algae living in the underlying water. This effect seems to be well reflected by the very low Chl-a concentrations in the seawater below the ice (Fig. 2c), which also agreed with the average concentration reported for the Arctic Ocean (Lee et al., 2015). The high Chl-a measured in the sea ice supports the elevated autotrophic activity within the ice brines and the roles of the
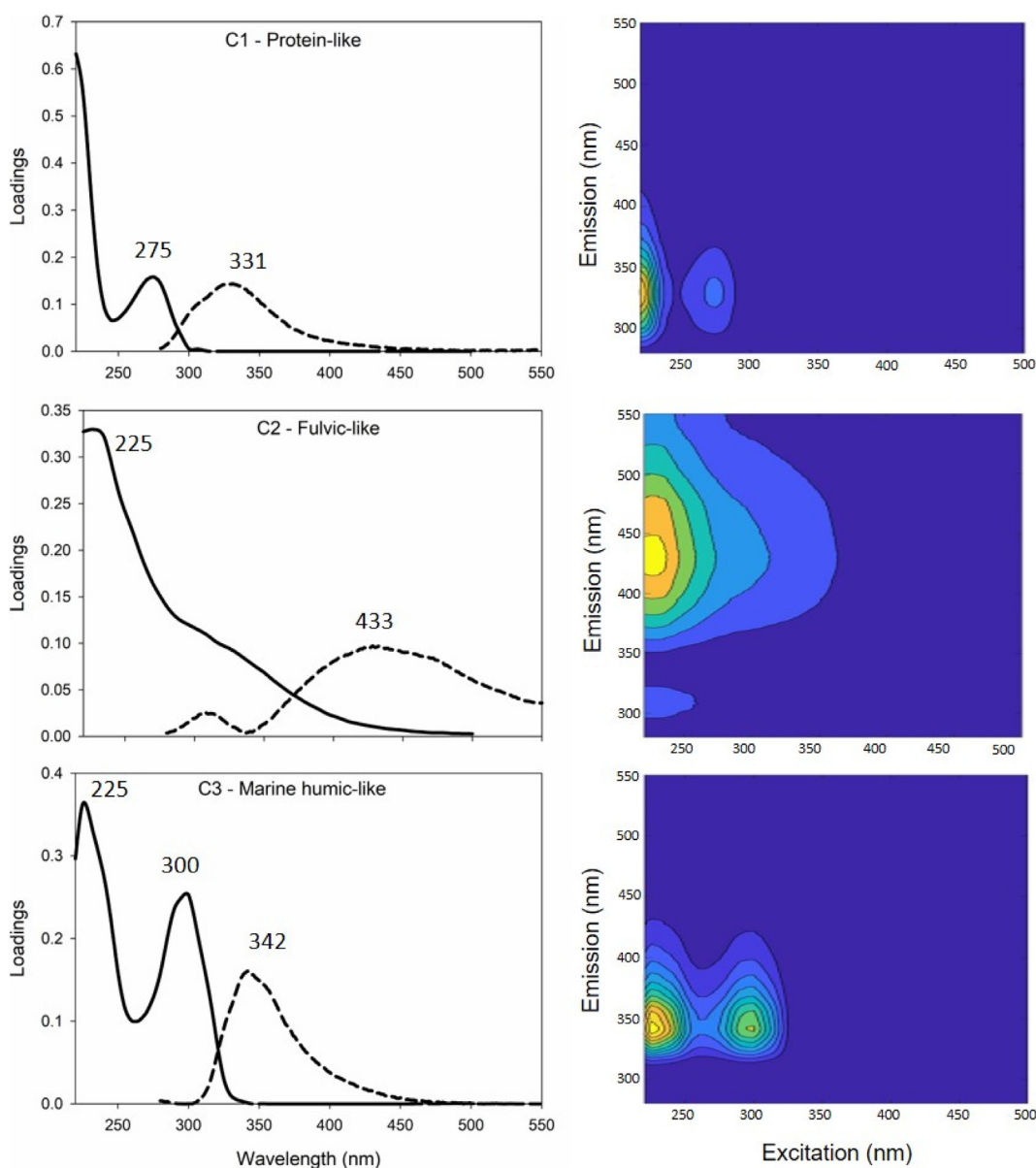

Fig. 3. Excitation (line) and emission (dashed line) spectra of the three fluorescent components validated by Parallel Factor analysis, PARAFAC (left) and their contour plots (right). The numbers indicate the maximum wavelength of each spectrum.

algal communities in DOC production. However, there was a lack of linear relationship between DOC and Chl-a in this study, implying the presence of other sources of DOC. The most probable source would be the microbial community, which can be very active in ice (Deming, 2009; Eronen-Rasimus et al., 2014) and is known to contribute up to 60% of total sea ice carbon (Riedel et al., 2008).

3.2. Comparison of FDOM components between the ice and the seawater

The elaboration of the EEMs with PARAFAC modeling resulted in the validation of a 3-component model (Fig. 3). In order to identify the FDOM components, the spectra were compared with (i) the matching spectra obtained from the OpenFluor database (Murphy et al., 2014) using the OpenFluor plugin for OpenChrom with a similarity score > 96%, and with (ii) other similar components reported in previous literature (Table S3). The spectral features of component 1 (C1, Ex/Em: 275/331 nm) are typical of protein-like substances, in particular tryptophan. This component was previously reported in sea ice (Hill and Zimmerman, 2016; Logvinova et al., 2016) as well as in other environments such as the open ocean, coastal areas, and rivers (Dainard et al., 2015; Guéguen et al., 2014; Yao et al., 2016). The component is usually attributed to an autochthonous substance. The spectral characteristics of component 2 (C2, Ex/Em: 225/433 nm) were related to the presence of terrestrial materials (Ishii and Boyer, 2012; Lambert et al., 2016; Shutova et al., 2014; Stedmon et al., 2011). In Arctic sea ice, Logvinova et al. (2016) assigned this component to fulvic-like material, while Hill and Zimmerman (2016) attributed these fluorescence characteristics to marine humic-like substances. In this study, C2 seems to be closer to fulvic-like components since the marine humic-like peak typically has a shorter emission maximum (peak M, Ex/Em: 290–310/370–410 nm, Coble, 2007). The spectral characteristics (Ex/Em: 225(300)/342 nm) of component 3 (C3) are likely related to the presence of proteinaceous materials based on the previous literature (Amaral et al., 2016; Catalá et al., 2015; Hill and Zimmerman, 2016; Stedmon et al., 2011, 2007). The maxima of C3 appear at longer wavelengths compared to C1, although the source of both components is similar.

Compared with those reported for the Canadian Arctic Ocean (Guéguen et al., 2012; Walker et al., 2009), our EEM-PARAFAC results presented a lower number of fluorescent components probably due to the lower abundance of humic-like substances. To discuss the relative contribution of each component, its maximum fluorescence intensity (F_{max}) was divided by the sum of the three (i.e., total fluorescence or Ftot = C1 + C2 + C3). Among the three components, the protein-like C1 exhibited the highest fluorescence intensity for this study (Fig. 4a), occupying 47–80% and 35–63% of the total fluorescence (Ftot) in the sea ice and the seawater, respectively, and C3 was responsible for 14–48% and 20–49% of the Ftot in each. Meanwhile, the fulvic-like C2 constituted the lower proportions with 4–14% in the ice and 8–30% in the seawater.

These results indicate that, both in the ice and in the seawater, autochthonous protein-like substances are more abundant than the terrestrial counterparts, agreeing with previous studies on sea ice. For example, Hill and Zimmerman (2016), in a study of the Canadian Arctic, observed that humic-like fluorescence represented only 8% of Ftot in the ice and 18% in the seawater below ice. Stedmon et al. (2011) found a dominant protein-like fluorescence in sea ice samples from the Antarctic.

For this study, C1 was significantly higher in the ice versus the seawater DOM ($p < 0.05$). In contrast, no statistical difference was found for the other two FDOM components (Fig. 4b and c), suggesting C2 and C3 may have the origins from the parent seawater. The highest abundance of C1 in the ice can be attributed to the production/release from phytoplankton and ice algae. However, no significant linear relationship was observed between Chl-a and C1 for this study (Fig. S4), signifying that other organisms could also play a role in the release of the protein-like substances. For example, the microbial community may be involved in the release of the protein-like fluorescence, as demonstrated by Elliott et al. (2006), who observed the production of tryptophan- and tyrosine-like compounds from a bacterial culture isolated from an urban river. Production of a tryptophan-like material was observed also in marine coastal areas (Retelletti Brogi et al., 2015).

3.3. Distributions of different size fractions in the ice and the seawater

The representative SEC chromatograms are shown in Fig. S5. The LMWA fraction is not reported here because its concentration was not detectable by the instrument. Among the remaining four different size fractions, the BP fraction, with the highest molecular weight, exhibited the lowest abundance both in the ice and in seawater (2–4%, Fig. 5).

The SEC result is somewhat in contrast with previous studies, which reported the production of a high amount of biopolymers (i.e., polysaccharides) by ice algae and microorganisms as a protection mechanism to the harshness of the ice environment (Krembs et al., 2011; Underwood et al., 2013, 2010). The very low presence of BP in this study may be attributed to the aggregation of biopolymers into molecules larger than 0.7 μm, and/or their high bioavailability (Baghoth et al., 2008; Dittmar and Kattner, 2003; Penru et al., 2013). Once the BP fraction is produced, it can be removed and/or reduced into smaller size compounds upon microbial activity. The HS fraction was more abundant in the seawater than in the ice cores, representing 27–42% and 8–12% of DOC, respectively (Fig. 5). The difference indicates that the seawater is much more affected by terrestrial sources in the DOM compared to the ice. The relative differences in the abundances were the opposite for the BB fraction, representing 12–21% and 22–27% of DOC in the seawater and the ice, respectively (Fig. 5). Considering that this fraction reflects the presence of low molecular weight HS, mostly derived from the breakdown of HS (Huber et al., 2011), the higher abundance of BB in the ice, in correspondence with a lower abundance of HS, implies higher microbial activity degrading HS into smaller BB in the ice versus seawater. The fraction of LMWN was the most abundant fraction, representing 63–69% of DOC in the ice and 36–51% of DOC in the seawater (Fig. 5). The LMWN fraction includes alcohols, aldehydes, ketones, sugars, and amino acids (Huber et al., 2011), which are known to be the byproduct of BP, HS, and BB degradation (Liu et al., 2010; Penru et al., 2013). Again, its high abundance in both the ice and seawater suggests the presence of an active microbial community that removes and
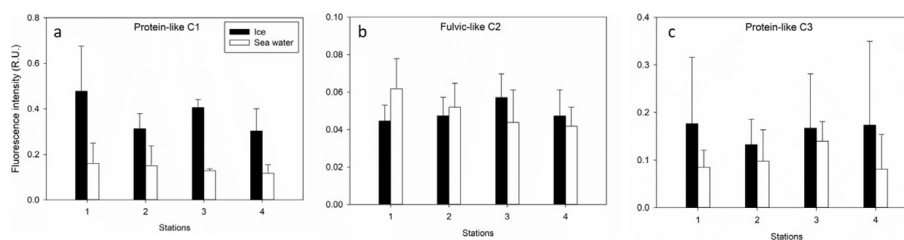

Fig. 4. Components 1 (a), 2 (b), and 3 (c) fluorescence in the four stations, in the ice (black) and seawater (white). Error bars refer to the standard deviations of the samples collected on 5 different sampling days.
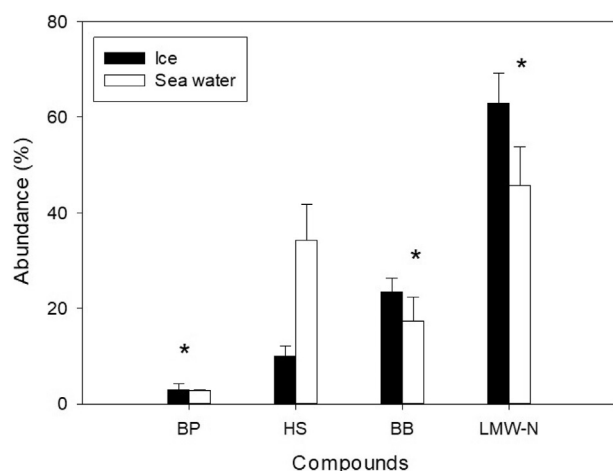
Fig. 5. Relative abundances of DOM size fractions (see text for more explanation on the abbreviation) in the ice (black) and the seawater (white). Error bars refer to the standard deviation of the samples collected at the four different stations. The asterisks highlight the size fractions which exhibit statistically significant differences between ice and sea water (Kruskal-Wallis test, $p < 0.05$).

"transforms" DOM into smaller sized compounds. This observation is in agreement with Stedmon et al. (2007), who attributed the decoupling between DOC and DON concentrations and the autochthonous protein-like fluorescence of ice samples to the presence of an active microbial community cycling labile autochthonous sub-fraction of DOM, which is thus difficult to detect using chemical measurements.

3.4. DOM accumulation in sea ice

To highlight in situ production within the ice, the accumulated DOM (DOM_{acc}) in ice was calculated by normalizing it to salinity (Müller et al., 2013; Stedmon et al., 2011) using the following formula:

$$DOM_{acc} = DOM_{ice} - \left(\frac{DOM_{sw}}{S_{sw}} S_{ice}\right)$$

where S_{sw} and S_{ice} are the values of salinity in seawater and ice, respectively. This calculation was applied only for DOC, C1, and the size fractions, which are the DOM parameters with significant differences between the ice and the underlying seawater. The enrichment factor
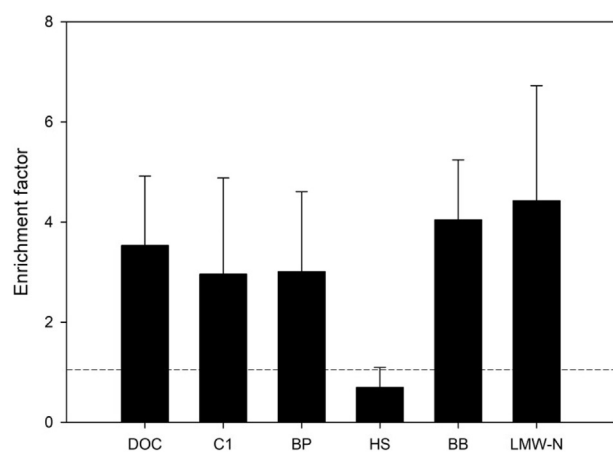
(EF) was then calculated as the ratio between the DOM_{acc} and the DOM in the seawater. If EF > 1, the relative parameter can be considered enriched in the ice with respect to the sea water, if EF < 1 it can be considered depleted. As a result, the EF of DOC ranged between 3.3 and 6.2 (Fig. 6), and the accumulated DOC represented the 89–97% (average 93%) of the ice DOC, which suggests that most of the DOC in the sea ice is produced in situ by biological activity.

These results are in good agreement with the EF values observed in the Weddell Sea (Norman et al., 2011). However, the calculated DOC_{acc} percentages here were higher than those reported for the Weddell Sea ice brines (average DOC_{acc} 61%) by Stedmon et al. (2011). The EF values of C1 ranged between 1.7 and 4.5 (Fig. 6), and the accumulated fluorescence represented 75–97% (average 89%) of the C1 fluorescence in the ice, confirming that the protein-like fluorescence originates mainly from in situ biological activity. The accumulation of protein-like fluorescence was also reported for the Baltic Sea (Müller et al., 2011) and Weddell Sea (Stedmon et al., 2011) but with lower EF values, revealing relatively a higher biological activity in our studied area.

All DOM size fractions were more enriched in the ice versus the seawater, except for HS which seems to remain constant (EF ≈ 1, Fig. 6). The LMWN had a high enrichment factor, probably because it contains the degraded byproducts of all other fractions. It is interesting to observe that, despite its low concentrations (Table S2), BP has a high enrichment factor. The accumulated BP represents 92–96% of the BP in ice. The production of BP in the ice may be explained largely by the production of extracellular polymeric substances (EPS) by algae and microorganisms as a defense mechanism to the extreme ice conditions (high salinity and low temperature). Similar to DOC, the accumulated amounts of the three size fractions (BP, BB, and LMWN) were 87–96% of the corresponding concentrations in the ice, suggesting again the origins of these compounds from the in situ production.

Recent studies reported an increasing trend in the ice that melts seasonally (Kinnard et al., 2011), and prediction models suggest that the Arctic Ocean would become seasonally nearly sea ice free before 2050 (Overland et al., 2014). This long-term prospect signifies that every year this large amount of biologically produced ice DOM would be released into the surface waters once the ice begins to melt. The DOM released into the seawater can be transported into the deep waters circulation system, or it can be assimilated by the microbial community and then converted into biomass or respired as CO_2. Despite this important implication, there were only two studies on the bioavailability of ice DOM (Amon et al., 2001; Jørgensen et al., 2015), which suggested that ice DOM might be more bioavailable than the seawater counterpart. Unfortunately, however, these studies relied on amended samples (Amon et al., 2001) or ice grown under laboratory conditions (Jørgensen et al., 2015) for demonstration. Further experiments should be therefore carried out, using un-amended natural sea ice and the seawater microbial community, in order to confirm these results and investigate the fate of ice DOM once the ice melts into the seawater.

3.5. Comparison of the molecular composition between the ice and the seawater – FT-ICR-MS

Mass spectra were analyzed in the m/z range of 200–800. A total of 563 and 580 formulas were assigned to the measured m/z values of the composite samples of the ice and the seawater, respectively, which corresponded to 41% and 33% of the peaks. The number of formulas was low compared to the previous studies on seawater (Dittmar and Koch, 2006; Flerus et al., 2012; Hertkorn et al., 2013), glacial ice (Bhatia et al., 2010; Grannas et al., 2006) and sea ice (Longnecker, 2015). The low number of formulas could be attributed to: (i) the low volume of the sample used for the SPE (approximately 0.5 L); (ii) potential instrumental interference occurring during ESI to alter the ionization, such as the formation of adducts, in-source fragmentation, or selective ionization (Reemtsma, 2009; Sleighter and Hatcher, 2011). It is notable that, due to the differences in extraction techniques, mass spectrometers,

Fig. 6. Enrichment factors (EF) of different DOM parameters (see text for more explanation on the abbreviations). Error bars refer to the standard deviations of the samples collected on five different days (DOC and C1) or at four different stations (BP, HS, BB, and LMWN). The horizontal dashed line highlights an EF value of 1.0.
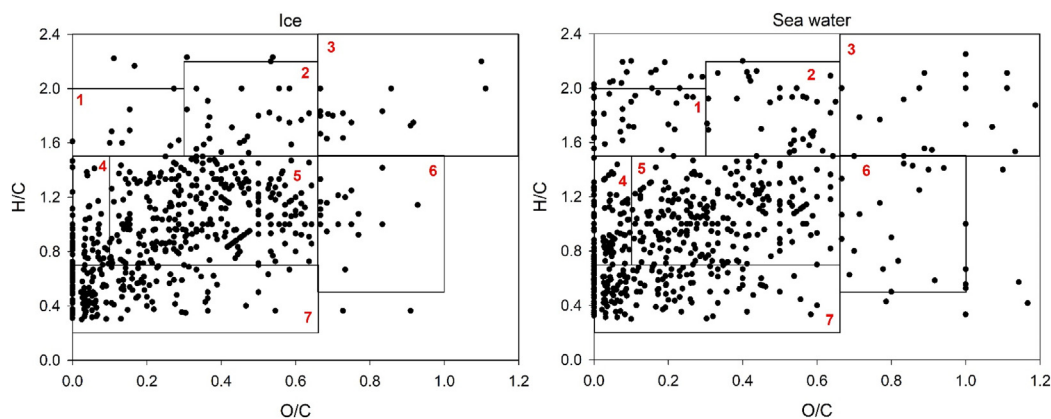
Fig. 7. van Krevelen diagram of the ice (left) and seawater (right) samples. The squares represent sub-division across 7 compound classes: lipids (1), proteins (2), carbohydrates (3), unsaturated hydrocarbons (4), lignin (5), tannins (6), and condensed aromatic structures (7).

and data processing, a direct comparison of the data with previous literature should be avoided (Longnecker, 2015; Reemtsma, 2009). In addition, the previous studies reporting the FT-ICR-MS results of ice samples all focused on different types of ice. For example, Grannas et al. (2006) studied the molecular composition of "old" glacial ice (from 1300 and 1950 CE). Bhatia et al. (2010) highlighted the differences between subglacial, supraglacial, snow, and tarn using melted water samples. Longnecker (2015) presented the results of first year sea ice characterized by a low primary production. Nevertheless, a broad comparison of the general features was made in this study.

The calculated formulas are displayed in the van Krevelen diagram (Kim et al., 2003) and are divided into 7 compound categories (lipids, proteins, carbohydrates, unsaturated hydrocarbons, lignin/CRAM, tannins and condensed aromatic structures, CAS) based on the literature (Hockaday et al., 2009; Hodgkins et al., 2016; Koch and Dittmar, 2006; Ohno et al., 2010; Stubbins et al., 2014; Willoughby et al., 2014).

In this study, the formulas of both the ice and the seawater samples were distributed over all of the compound categories (Fig. 7), which was also observed when the different heteroatoms were taken into account (Fig. S6). The results are in agreement with those of the Arctic subglacial samples (Bhatia et al., 2010) and first year sea ice (Longnecker, 2015). A marked difference was instead observed compared to the data reported by Grannas et al. (2006), who highlighted a predominance of formulas in the lipid/lignin area of the van Krevelen diagram of 'old' glacial ice. Looking in detail at the distribution of the formulas, it was possible to observe some differences between the ice and the seawater. In the seawater, slightly higher percentages of lipids and unsaturated hydrocarbons were observed, while there was a higher abundance of lignin in the ice (Table 1).

In both samples, most of the formulas are representative of lignin/CRAM-like (>38%) and CAS-like (>25%) compounds. The highest abundance of lignin/CRAM-like formulas is in line with Bhatia et al. (2010), in which terrestrial sourced formulas (in the same region where lignin/CRAM is assigned here) exhibited the highest abundance in subglacial ice samples (>39%), although they observed a markedly higher abundance of protein-like formulas than the results of this study. Meanwhile, the high percentage of CAS-like formulas agreed with Longnecker (2015).

The elemental formulas containing C, H, O, and N dominated both types of samples, followed by the formulas of C, H, and O in the ice, and the formulas of C, H, N, O, and S in the seawater (Table 1). Compared to the previous studies reporting greater abundances of the C/H/O formulas (Bhatia et al., 2010; Longnecker, 2015), the samples in this study showed a higher percentage of nitrogen-containing formulas. It has yet to be taken into account that nitrogen-containing molecules may vary between similar studies due to extraction biases (Reemtsma, 2009) and different procedures in formula assignments. Meanwhile, some other parameters such as the intensity normalized elemental ratios, the double bond equivalent (DBE), and the modified aromatic index (Koch and Dittmar, 2006), showed similar values between the two samples (Table S2). However, it is noteworthy that the m/z values revealed only 32 identical formulas ($\approx 5.5\%$ of total formulas) assigned to both types of samples. Longnecker (2015) also observed very little overlap of m/z values between seawater and some of the sea ice samples. Almost all the overlapping formulas fall within the range of lignin/CRAM compounds. This compound group may represent the terrigenous refractory materials that can be partially trapped within the ice. Similar formulas are considered to represent refractory materials (Flerus et al., 2012; Gonsior et al., 2011; Koch et al., 2005).

These findings suggest that, although no major differences were found in the apparent molecular indices between ice and seawater DOM, the sources of the DOM could differ between the two, supporting a greater role of in situ production in forming ice DOM. Furthermore, these results point out the need for more detailed studies, which should include a higher number of samples, to investigate deeper the molecular differences between ice and seawater DOM.

4. Conclusions

This study combined all DOM information on the concentrations, optical properties, molecular size distribution, and the molecular formulas for the comparison between Arctic sea ice and the underlying seawater. This combination of analytical techniques allowed, for the first time, to characterize DOM in various aspects, confirming most of the previously reported information on sea ice DOM. The high DOC enrichment factor highlights that most DOM is likely produced in situ, and subsequently

Table 1
Percentages (%) of the different compounds-like and heteroatoms formulas in ice and sea water samples (the abbreviations used are explained in the text).

	Lipids	Protein	Carbohydrates	Unsaturated hydrocarbons	Lignin	Tannins	CAS	CHO	CHON	CHOS	CHNOS
Ice	2	6	2	11	50	4	26	28	38	9	15
Sea Water	6	6	3	15	38	4	27	16	42	11	18

accumulated via a decoupling of its production and removal processes. The relatively higher abundances of Chl-a and protein-like fluorescence in the ice versus the seawater suggest that the ice DOM may be produced by both the autotrophic and heterotopic communities. More enrichment of DOM size fractions in the ice, except for the HS fraction, confirmed the in situ production of DOM. A small portion of the number of the overlapped formulas between the ice and the seawater imply differing DOM sources and properties with respect to the main sources, although the apparent molecular indices were similar. This study provided a new insight into the possible increase in autochthonous (probably labile) DOM release from Arctic seasonal sea ice melting under climate change conditions. However, for more concrete evidence, comparative biodegradation experiments are warranted in the future using ice and seawater samples, which would clarify the lability of ice DOM and the future impacts on DOM composition in the Arctic Ocean environment.

Acknowledgments

Competing financial interests

The authors declare no competing financial interests.

Appendix A. Supplementary information

Statistical summary of all measured parameters, PARAFAC components peaks summary and comparison with literature, SEC-OCD spectra for ice and seawater samples, and van Krevelen diagrams highlighting the different heteroatoms can be found here. Supplementary data associated with this article can be found in the online version, at doi: https://doi.org/10.1016/j.scitotenv.2018.01.251.

References

Amaral, V., Graeber, D., Calliari, D., Alonso, C., 2016. Strong linkages between DOM optical properties and main clades of aquatic bacteria. Limnol. Oceanogr. 61:906–918. https://doi.org/10.1002/lno.10258.

Amon, R.M.W., Fitznar, H.-P., Benner, R., 2001. Linkages among the bioreactivity, chemical composition, and diagenetic state of marine dissolved organic matter. Limnol. Oceanogr. 46:287–297. https://doi.org/10.4319/lo.2001.46.2.0287.

Anderson, L.G., 2002. DOC in the Arctic Ocean. In: Hansell, D.A., Carlson, C.A. (Eds.), Biogeochemistry of Marine Dissolved Organic Matter, pp. 665–706.

Anderson, L.G., Amon, R.M.W., 2015. DOM in the Arctic Ocean. Biogeochemistry of Marine Dissolved Organic Matter: Second Edition:pp. 609–633 https://doi.org/10.1016/B978-0-12-405940-5.00014-5.

Arrigo, K.R., 2016. Sea ice as a habitat for primary producers. Sea Ice: Third Edition: pp. 352–369 https://doi.org/10.1002/9781118778371.ch14.

Aslam, S.N., Underwood, G.J.C., Kaartokallio, H., Norman, L., Autio, R., Fischer, M., Kuosa, H., Dieckmann, G.S., Thomas, D.N., 2012. Dissolved extracellular polymeric substances (dEPS) dynamics and bacterial growth during sea ice formation in an ice tank study. Polar Biol. 35:661–676. https://doi.org/10.1007/s00300-011-1112-0.

Baghoth, S.A., Maeng, S.K., Rodríguez, S.G.S., Ronteltap, M., Sharma, S., Kennedy, M., Amy, G.L., 2008. An urban water cycle perspective of natural organic matter (NOM): NOM in drinking water, wastewater effluent, storm water, and seawater. Water Sci. Technol. Water Supply 8:701. https://doi.org/10.2166/ws.2008.146.

Benner, R., Louchouarn, P., Amon, R.M.W., 2005. Terrigenous dissolved organic matter in the Arctic Ocean and its transport to surface and deep waters of the North Atlantic. Glob. Biogeochem. Cycles 19. https://doi.org/10.1029/2004GB002398.

Bhatia, M.P., Das, S.B., Longnecker, K., Charette, M.A., Kujawinski, E.B., 2010. Molecular characterization of dissolved organic matter associated with the Greenland ice sheet. Geochim. Cosmochim. Acta 74:3768–3784. https://doi.org/10.1016/j.gca.2010.03.035.

Carlson, C.A., Hansell, D.A., 2015. DOM sources, sinks, reactivity, and budgets. Biogeochemistry of Marine Dissolved Organic Matter:pp. 65–126 https://doi.org/10.1016/B978-0-12-405940-5.00003-0.

Catalá, T.S., Reche, I., Fuentes-Lema, A., Romera-Castillo, C., Nieto-Cid, M., Ortega-Retuerta, E., Calvo, E., Álvarez, M., Marrasé, C., Stedmon, C.A., Álvarez-Salgado, X.A., 2015. Turnover time of fluorescent dissolved organic matter in the dark global ocean. Nat. Commun. 6 (5986). https://doi.org/10.1038/ncomms6986.

Chen, M., He, W., Choi, I., Hur, J., 2016a. Tracking the monthly changes of dissolved organic matter composition in a newly constructed reservoir and its tributaries during the initial impounding period. Environ. Sci. Pollut. Res. 23:1274–1283. https://doi.org/10.1007/s11356-015-5350-5.

Chen, M., Kim, S., Park, J.-E., Jung, H.-J., Hur, J., 2016b. Structural and compositional changes of dissolved organic matter upon solid-phase extraction tracked by multiple analytical tools. Anal. Bioanal. Chem. 408:6249–6258. https://doi.org/10.1007/s00216-016-9728-0.

Coble, P.G., 2007. Marine optical biogeochemistry: the chemistry of ocean color. Chem. Rev. 107:402–418. https://doi.org/10.1021/cr050350+.

Dainard, P.G., Guéguen, C., McDonald, N., Williams, W.J., 2015. Photobleaching of fluorescent dissolved organic matter in Beaufort Sea and North Atlantic subtropical gyre. Mar. Chem. 177:630–637. https://doi.org/10.1016/j.marchem.2015.10.004.

Deming, J.W., 2009. Sea Ice Bacteria and Viruses, in: Sea Ice: An Introduction to Its Physics. Chemistry, Biology, and Geology:247–282 https://doi.org/10.1002/9781444317145.

Derrien, M., Lee, Y.K., Hur, J., 2017a. Comparing the spectroscopic and molecular characteristics of different dissolved organic matter fractions isolated by hydrophobic and anionic exchange resins using fluorescence spectroscopy and FT-ICR-MS. WaterSA 9:555. https://doi.org/10.3390/w9080555.

Derrien, M., Lee, Y.K., Park, J.E., Li, P., Chen, M., Lee, S.H., Lee, S.H., Lee, J.B., Hur, J., 2017b. Spectroscopic and molecular characterization of humic substances (HS) from soils and sediments in a watershed: comparative study of HS chemical fractions and the origins. Environ. Sci. Pollut. Res. 24:16933–16945. https://doi.org/10.1007/s11356-017-9225-9.

Dittmar, T., Kattner, G., 2003. Recalcitrant dissolved organic matter in the ocean: major contribution of small amphiphilics. Mar. Chem. 82:115–123. https://doi.org/10.1016/S0304-4203(03)00068-9.

Dittmar, T., Koch, B.P., 2006. Thermogenic organic matter dissolved in the abyssal ocean. Mar. Chem. 102:208–217. https://doi.org/10.1016/j.marchem.2006.04.003.

Dittmar, T., Koch, B., Hertkorn, N., Kattner, G., 2008. A simple and efficient method for the solid-phase extraction of dissolved organic matter (SPE-DOM) from seawater. Limnol. Oceanogr. Methods 6:230–235. https://doi.org/10.4319/lom.2008.6.230.

Ehn, J., Granskog, M.A., Reinart, A., Erm, A., 2004. Optical properties of melting landfast sea ice and underlying seawater in Santala Bay, Gulf of Finland. J. Geophys. Res. C Ocean. 109:1–12. https://doi.org/10.1029/2003JC002042.

Elliott, S., Lead, J.R., Baker, A., 2006. Characterisation of the fluorescence from freshwater, planktonic bacteria. Water Res. 40:2075–2083. https://doi.org/10.1016/j.watres.2006.03.017.

Eronen-Rasimus, E., Kaartokallio, H., Lyra, C., Autio, R., Kuosa, H., Dieckmann, G.S., Thomas, D.N., 2014. Bacterial community dynamics and activity in relation to dissolved organic matter availability during sea-ice formation in a mesocosm experiment. Microbiology 3:139–156. https://doi.org/10.1002/mbo3.157.

Flerus, R., Lechtenfeld, O.J., Koch, B.P., McCallister, S.L., Schmitt-Kopplin, P., Benner, R., Kaiser, K., Kattner, G., 2012. A molecular perspective on the ageing of marine dissolved organic matter. Biogeosciences 9:1935–1955. https://doi.org/10.5194/bg-9-1935-2012.

Gonsior, M., Peake, B.M., Cooper, W.T., Podgorski, D.C., D'Andrilli, J., Dittmar, T., Cooper, W.J., 2011. Characterization of dissolved organic matter across the subtropical convergence off the South Island, New Zealand. Mar. Chem. 123:99–110. https://doi.org/10.1016/J.MARCHEM.2010.10.004.

Grannas, A.M., Hockaday, W.C., Hatcher, P.G., Thompson, L.G., Mosley-Thompson, E., 2006. New revelations on the nature of organic matter in ice cores. J. Geophys. Res. Atmos. 111:1–10. https://doi.org/10.1029/2005JD006251.

Granskog, M.A., Kaartokallio, H., Thomas, D.N., Kuosa, H., 2005. Influence of freshwater inflow on the inorganic nutrient and dissolved organic matter within coastal sea ice and underlying waters in the Gulf of Finland (Baltic Sea). Estuar. Coast. Shelf Sci. 65:109–122. https://doi.org/10.1016/j.ecss.2005.05.011.

Guéguen, C., McLaughlin, F.A., Carmack, E.C., Itoh, M., Narita, H., Nishino, S., 2012. The nature of colored dissolved organic matter in the southern Canada Basin and East Siberian Sea. Deep. Res. Part II Top. Stud. Oceanogr. 81–84:102–113. https://doi.org/10.1016/j.dsr2.2011.05.004.

Guéguen, C., Cuss, C.W., Cassels, C.J., Carmack, E.C., 2014. Absorption and fluorescence of dissolved organic matter in the waters of the Canadian Arctic archipelago, Baffin Bay, and the Labrador Sea. J. Geophys. Res. Oceans 119:2034–2047. https://doi.org/10.1002/2013JC009173.

He, W., Chen, M., Park, J.E., Hur, J., 2016. Molecular diversity of riverine alkaline-extractable sediment organic matter and its linkages with spectral indicators and molecular size distributions. Water Res. 100:222–231. https://doi.org/10.1016/j.watres.2016.05.023.

Hertkorn, N., Harir, M., Koch, B.P., Michalke, B., Schmitt-Kopplin, P., 2013. High-field NMR spectroscopy and FTICR mass spectrometry: powerful discovery tools for the molecular level characterization of marine dissolved organic matter. Biogeosciences 10: 1583–1624. https://doi.org/10.5194/bg-10-1583-2013.

Hill, V.J., Zimmerman, R.C., 2016. Characteristics of colored dissolved organic material in first year landfast sea ice and the underlying water column in the Canadian Arctic in the early spring. Mar. Chem. 180:1–13. https://doi.org/10.1016/j.marchem.2016.01.007.

Hockaday, W.C., Purcell, J.M., Marshall, A.G., Baldock, J.A., Hatcher, P.G., 2009. Electrospray and photoionization mass spectrometry for the characterization of organic matter in natural waters: a qualitative assessment. Limnol. Oceanogr. Methods 7:81–95. https://doi.org/10.4319/lom.2009.7.81.

Hodgkins, S.B., Tfaily, M.M., Podgorski, D.C., McCalley, C.K., Saleska, S.R., Crill, P.M., Rich, V.I., Chanton, J.P., Cooper, W.T., 2016. Elemental composition and optical properties reveal changes in dissolved organic matter along a permafrost thaw chronosequence in

a subarctic peatland. Geochim. Cosmochim. Acta 187:123–140. https://doi.org/10.1016/j.gca.2016.05.015.

Huber, S.A., Balz, A., Abert, M., Pronk, W., 2011. Characterisation of aquatic humic and non-humic matter with size-exclusion chromatography e organic carbon detection e organic nitrogen detection (LC-OCD-OND). Water Res. 45:879–885. https://doi.org/10.1016/j.watres.2010.09.023.

Hur, J., Hwang, S.-J., Shin, J.-K., 2008. Using synchronous fluorescence technique as a water quality monitoring tool for an Urban River. Water Air Soil Pollut. 191: 231–243. https://doi.org/10.1007/s11270-008-9620-4.

Ishii, S., Boyer, T., 2012. Behavior of reoccurring PARAFAC components in fluorescent dissolved organic matter in natural and engineered systems: a critical review. Environ. Sci. Technol. 46, 2006–2017.

Jiao, N., Herndl, G.J., Hansell, D.A., Benner, R., Kattner, G., Wilhelm, S.W., Kirchman, D.L., Weinbauer, M.G., Luo, T., Chen, F., Azam, F., 2010. Microbial production of recalcitrant dissolved organic matter: long-term carbon storage in the global ocean. Nat. Rev. Microbiol. 8:593–599. https://doi.org/10.1038/nrmicro2386.

Jørgensen, L., Stedmon, C.A., Kaartokallio, H., Middelboe, M., Thomas, D.N., 2015. Changes in the composition and bioavailability of dissolved organic matter during sea ice formation. Limnol. Oceanogr. 60:817–830. https://doi.org/10.1002/lno.10058.

Junge, K., Eicken, H., Deming, J.W., 2004. Bacterial activity at −2 to −20 degrees C in Arctic wintertime sea ice. Appl. Environ. Microbiol. 70:550–557. https://doi.org/10.1128/AEM.70.1.550.

Kaartokallio, H., Kuosa, H., Thomas, D.N., Granskog, M.A., Kivi, K., 2007. Biomass, composition and activity of organism assemblages along a salinity gradient in sea ice subjected to river discharge in the Baltic Sea. Polar Biol. 30:183–197. https://doi.org/10.1007/s00300-006-0172-z.

Kim, S., Kramer, R.W., Hatcher, P.G., 2003. Graphical method for analysis of ultrahigh-resolution broadband mass spectra of natural organic matter, the Van Krevelen diagram. Anal. Chem. 75:5336–5344. https://doi.org/10.1021/ac034415p.

Kinnard, C., Zdanowicz, C.M., Fisher, D.A., Isaksson, E., de Vernal, A., Thompson, L.G., 2011. Reconstructed changes in Arctic sea ice over the past 1,450 years. Nature 479: 509–512. https://doi.org/10.1038/nature10581.

Koch, B.P., Dittmar, T., 2006. From mass to structure: an aromaticity index for high-resolution mass data of natural organic matter. Rapid Commun. Mass Spectrom. 20: 926–932. https://doi.org/10.1002/rcm.2386.

Koch, B.P., Witt, M., Engbrodt, R., Dittmar, T., Kattner, G., 2005. Molecular formulae of marine and terrigenous dissolved organic matter detected by electrospray ionization Fourier transform ion cyclotron resonance mass spectrometry. Geochim. Cosmochim. Acta 69:3299–3308. https://doi.org/10.1016/J.GCA.2005.02.027.

Koch, B.P., Ludwichowski, K.U., Kattner, G., Dittmar, T., Witt, M., 2008. Advanced characterization of marine dissolved organic matter by combining reversed-phase liquid chromatography and FT-ICR-MS. Mar. Chem. 111:233–241. https://doi.org/10.1016/j.marchem.2008.05.008.

Krembs, C., Eicken, H., Deming, J.W., 2011. Exopolymer alteration of physical properties of sea ice and implications for ice habitability and biogeochemistry in a warmer Arctic. Proc. Natl. Acad. Sci. 108:3653–3658. https://doi.org/10.1073/pnas.1100701108.

Lambert, T., Bouillon, S., Darchambeau, F., Massicotte, P., Borges, A.V., 2016. Shift in the chemical composition of dissolved organic matter in the Congo River network. Biogeosciences 13:5405–5420. https://doi.org/10.5194/bg-13-5405-2016.

Lee, Y.J., Matrai, P.A., Friedrichs, M.A.M., Saba, V.S., Antoine, D., Ardyna, M., Asanuma, I., Babin, M., Bélanger, S., Benoît-Gagné, M., Devred, E., Fernández-Méndez, M., Gentili, B., Hirawake, T., Kang, S.H., Kameda, T., Katlein, C., Lee, S.H., Lee, Z., Mélin, F., Scardi, M., Smyth, T.J., Tang, S., Turpie, K.R., Waters, K.J., Westberry, T.K., 2015. An assessment of phytoplankton primary productivity in the Arctic Ocean from satellite ocean color/in situ chlorophyll-a based models. J. Geophys. Res. C: Oceans 120:6508–6541. https://doi.org/10.1002/2015JC011018.

Liu, S., Lim, M., Fabris, R., Chow, C.W.K., Drikas, M., Korshin, G., Amal, R., 2010. Multi-wavelength spectroscopic and chromatography study on the photocatalytic oxidation of natural organic matter. Water Res. 44:2525–2532. https://doi.org/10.1016/j.watres.2010.01.036.

Logvinova, C.L., Frey, K.E., Cooper, L.W., 2016. The potential role of sea ice melt in the distribution of chromophoric dissolved organic matter in the Chukchi and Beaufort seas. Deep. Res. Part II Top. Stud. Oceanogr. 130:28–42. https://doi.org/10.1016/j.dsr2.2016.04.017.

Longnecker, K., 2015. Dissolved organic matter in newly formed sea ice and surface seawater. Geochim. Cosmochim. Acta 171:39–49. https://doi.org/10.1016/j.gca.2015.08.014.

Meiners, K.M., Papadimitriou, S., Thomas, D.N., Norman, L., Dieckmann, G.S., 2009. Biogeochemical conditions and ice algal photosynthetic parameters in Weddell sea ice during early spring. Polar Biol. 32:1055–1065. https://doi.org/10.1007/s00300-009-0605-6.

Müller, S., Vähätalo, A.V., Granskog, M.A., Autio, R., Kaartokallio, H., 2011. Behaviour of dissolved organic matter during formation of natural and artificially grown Baltic sea ice. Ann. Glaciol. 52:233–241. https://doi.org/10.3189/172756411795931886.

Müller, S., Vähätalo, A.V., Stedmon, C.A., Granskog, M.A., Norman, L., Aslam, S.N., Underwood, G.J.C., Dieckmann, G.S., Thomas, D.N., 2013. Selective incorporation of dissolved organic matter during sea ice formation. Mar. Chem. 155: 148–157. https://doi.org/10.1016/j.marchem.2013.06.008.

Murphy, K.R., Butler, K.D., Spencer, R.G.M., Stedmon, C.A., Boehme, J.R., Aiken, G.R., 2010. Measurement of dissolved organic matter fluorescence in aquatic environments: an Interlaboratory comparison. Environ. Sci. Technol. 44:9405–9412. https://doi.org/10.1021/es102362t.

Murphy, K.R., Stedmon, C.A., Graeber, D., Bro, R., 2013. Fluorescence spectroscopy and multi-way techniques. PARAFAC. Anal. Methods 5:6557. https://doi.org/10.1039/c3ay41160e.

Murphy, K.R., Stedmon, C.A., Wenig, P., Bro, R., 2014. OpenFluor- an online spectral library of auto-fluorescence by organic compounds in the environment. Anal. Methods 6: 658–661. https://doi.org/10.1039/C3AY41935E.

Norman, L., Thomas, D.N., Stedmon, C.a., Granskog, M.A., Papadimitriou, S., Krapp, R.H., Meiners, K.M., Lannuzel, D., van der Merwe, P., Dieckmann, G.S., 2011. The characteristics of dissolved organic matter (DOM) and chromophoric dissolved organic matter (CDOM) in Antarctic sea ice. Deep-Sea Res. II Top. Stud. Oceanogr. 58:1075–1091. https://doi.org/10.1016/j.dsr2.2010.10.030.

Ohno, T., He, Z., Sleighter, R.L., Honeycutt, C.W., Hatcher, P.G., 2010. Ultrahigh resolution mass spectrometry and indicator species analysis to identify marker components of soil- and plant biomass-derived organic matter fractions. Environ. Sci. Technol. 44: 8594–8600. https://doi.org/10.1021/es101089t.

Overland, J.E., Wang, M., Walsh, J.E., Stroeve, J.C., 2014. Future Arctic climate changes: adaptation and mitigation time scales. Earth's Futur. 2:68–74. https://doi.org/10.1002/2013EF000162.

Parson, T.R., Maita, Y., Lalli, C.M., 1984. A Manual of Chemical and Biological Methods for Seawater Analysis. https://doi.org/10.1016/B978-0-08-030287-4.50002-5.

Penru, Y., Simon, F.X., Guastalli, A.R., Esplugas, S., Llorens, J., Baig, S., 2013. Characterization of natural organic matter from Mediterranean coastal seawater. J. Water Supply Res. Technol. - AQUA 62:42–51. https://doi.org/10.2166/aqua.2013.113.

Petrich, C., Eicken, H., 2010. Growth, Structure and Properties of Sea Ice. Sea Ice:23–78 https://doi.org/10.1002/9781444317145.ch2.

Pomeroy, L.R., Wiebe, W.J., 2001. Temperature and substrates as interactive limiting factors for marine heterotrophic bacteria. Aquat. Microb. Ecol. 23, 187–204.

Reemtsma, T., 2009. Determination of molecular formulas of natural organic matter molecules by (ultra-) high-resolution mass spectrometry. Status and needs. J. Chromatogr. A. https://doi.org/10.1016/j.chroma.2009.02.033.

Repeta, D.J., 2015. Chemical characterization and cycling of dissolved organic matter. Biogeochemistry of Marine Dissolved Organic Matter:pp. 21–63 https://doi.org/10.1016/B978-0-12-405940-5.00002-9.

Retelletti Brogi, S., Gonnelli, M., Vestri, S., Santinelli, C., 2015. Biophysical processes affecting DOM dynamics at the Arno river mouth (Tyrrhenian Sea). Biophys. Chem. 197, 1–9.

Riedel, A., Michel, C., Gosselin, M., LeBlanc, B., 2008. Winter-spring dynamics in sea-ice carbon cycling in the coastal Arctic Ocean. J. Mar. Syst. 74:918–932. https://doi.org/10.1016/j.jmarsys.2008.01.003.

Shutova, Y., Baker, A., Bridgeman, J., Henderson, R.K., 2014. Spectroscopic characterisation of dissolved organic matter changes in drinking water treatment: from PARAFAC analysis to online monitoring wavelengths. Water Res. 54:159–169. https://doi.org/10.1016/j.watres.2014.01.053.

Sipler, R.E., Bronk, D.A., 2015. Dynamics of dissolved organic nitrogen. Biogeochemistry of Marine Dissolved Organic Matter:pp. 127–232 https://doi.org/10.1016/B978-0-12-405940-5.00004-2.

Sleighter, R.L., Hatcher, P.G., 2011. Fourier transform mass spectrometry for the molecular level characterization of natural organic matter: instrument capabilities, applications, and limitations. Fourier Transforms - Approach to Scientific Principles:pp. 295–320 https://doi.org/10.5772/15959.

Smith, R.E.H., Gosselin, M., Kudoh, S., Robineau, B., Taguchi, S., 1997. DOC and its relationship to algae in bottom ice communities. J. Mar. Syst. 11:71–80. https://doi.org/10.1016/S0924-7963(96)00029-2.

Sokal, R.R., Rohlf, F.J., 1995. Biometry: the principles and practice of statistics in biological research. WH Freeman and Co., New York https://doi.org/papers2://publication/uuid/C017367B-5583-4EC4-BA2F-27E086259D21.

Stedmon, C.A., Thomas, D.N., Granskog, M., Kaartokallio, H., Papadimitriou, S., Kuosa, H., 2007. Characteristics of dissolved organic matter in baltic coastal sea ice: Allochthonous or autochthonous origins? Environ. Sci. Technol. 41:7273–7279. https://doi.org/10.1021/es071210f.

Stedmon, C.A., Thomas, D.N., Papadimitriou, S., Granskog, M.A., Dieckmann, G.S., 2011. Using fluorescence to characterize dissolved organic matter in Antarctic sea ice brines. J. Geophys. Res. Biogeosci. 116:1–9. https://doi.org/10.1029/2011JG001716.

Stubbins, A., Lapierre, J.-F.F., Berggren, M., Prairie, Y.T., Dittmar, T., del Giorgio, P.A., 2014. What's in an EEM? Molecular signatures associated with dissolved organic fluorescence in boreal Canada. Environ. Sci. Technol. 48:10598–10606. https://doi.org/10.1021/es502086e.

Thomas, D.N.D.D., Rubhn Lara, B.J., Kattner, Hajo Eicken Gerhard, Annelie Skoog, B., 1995. Dissolved organic matter in Arctic multi-year sea ice during winter: major components and relationship to ice characteristics. Polar Biology 15:477–483. https://doi.org/10.1007/BF00237461.

Thomas, D.N., Kattner, G., Engbrodt, R., Giannelli, V., Haas, C., Dieckmann, G.S., 2001. Dissolved organic matter in Antarctic sea ice. Ann. Glaciol. 33, 297–303.

Thomas, D.N., Papadimitriou, S., Michel, C., 2010. Biogeochemistry of Sea Ice. Sea Ice: Second Edition:pp. 425–467 https://doi.org/10.1002/9781444317145.ch12.

Underwood, G.J.C., Fietz, S., Papadimitriou, S., Thomas, D.N., Dieckmann, G.S., 2010. Distribution and composition of dissolved extracellular polymeric substances (EPS) in Antarctic sea ice. Mar. Ecol. Prog. Ser. 404:1–19. https://doi.org/10.2307/24873850.

Underwood, G.J.C., Aslam, S.N., Michel, C., Niemi, A., Norman, L., Meiners, K.M., Laybourn-Parry, J., Paterson, H., Thomas, D.N., 2013. Broad-scale predictability of carbohydrates and exopolymers in Antarctic and Arctic sea ice. Proc. Natl. Acad. Sci. 110: 15734–15739. https://doi.org/10.1073/pnas.1302870110.

Walker, S.A., Amon, R.M.W., Stedmon, C., Duan, S., Louchouarn, P., 2009. The use of PARAFAC modeling to trace terrestrial dissolved organic matter and fingerprint

water masses in coastal Canadian Arctic surface waters. J. Geophys. Res. Biogeosci. 114. https://doi.org/10.1029/2009JG000990.

Willoughby, A.S., Wozniak, A.S., Hatcher, P.G., 2014. A molecular-level approach for characterizing water-insoluble components of ambient organic aerosol particulates using ultrahigh-resolution mass spectrometry. Atmos. Chem. Phys. 14:10299–10314. https://doi.org/10.5194/acp-14-10299-2014.

Xie, H., Aubry, C., Zhang, Y., Song, G., 2014. Chromophoric dissolved organic matter (CDOM) in first-year sea ice in the western Canadian Arctic. Mar. Chem. 165: 25–35. https://doi.org/10.1016/j.marchem.2014.07.007.

Yao, B., Hu, C., Liu, Q., 2016. Fluorescent components and spatial patterns of chromophoric dissolved organic matters in Lake Taihu, a large shallow eutrophic lake in China. Environ. Sci. Pollut. Res. 23:23057–23070. https://doi.org/10.1007/s11356-016-7510-7.